Article

Nanomolar Protein Sensing with Embedded Receptor Molecules

Reza Zadmard, and Thomas Schrader

J. Am. Chem. Soc., **2005**, 127 (3), 904-915• DOI: 10.1021/ja045785d • Publication Date (Web): 31 December 2004

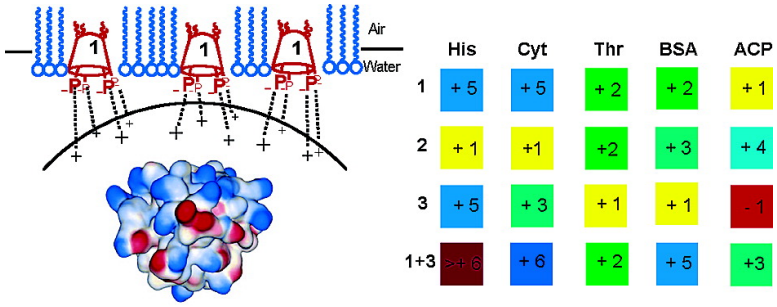

More About This Article

Additional resources and features associated with this article are available within the HTML version:

- Supporting Information
- Links to the 16 articles that cite this article, as of the time of this article download
- Access to high resolution figures
- Links to articles and content related to this article
- Copyright permission to reproduce figures and/or text from this article

View the Full Text HTML

J|A|C|S
ARTICLES
Published on Web 12/31/2004

Nanomolar Protein Sensing with Embedded Receptor Molecules

Reza Zadmard and Thomas Schrader*

Contribution from the Philipps-Universität Marburg, Fachbereich Chemie, Hans-Meerwein-Strasse, 35032 Marburg, Germany

Received July 14, 2004; E-mail: schradet@staff.uni-marburg.de

Abstract: A new concept of protein sensing at the air−water interface is introduced, based on amphiphilic receptor molecules embedded in a lipid monolayer. The process begins with incorporation of a small amount (0.13 equiv) of one or two different calix[4]arenes, adorned with charged functional groups at their upper rims, into a stearic acid monolayer. These doped monolayers are subsequently shown to attract peptides and proteins from the aqueous subphase. Depending on the host structure, the monolayers can be made selective for basic or acidic proteins. A working model is proposed, which explains the large observed p/A shifts with reincorporation of excess receptor molecules into the lipid monolayer after complex formation with the oppositely charged protein. This requires a self-assembly of multiple calixarene units over the protein surface, which bind the protein in a cooperative fashion. Oppositely charged calixarene derivatives do not form molecular capsules inside the monolayer, but rather remain separate inside the lipid layer, adopting a perpendicular orientation. They combine their hydrogen bond donor and acceptor capacities, and thus markedly enhance the sensitivity of the sensor system toward proteins, pushing the detection limits to 10 pM concentrations. The response pattern obtained from various receptor units inside the monolayer toward the same protein creates a fingerprint for this protein, which can hence be selectively detected at nanomolar concentrations (pattern recognition).

Introduction

The precise recognition of protein surfaces by other proteins is a prerequisite for numerous essential biological processes;[1] an instructive example is the self-assembly of viral coat proteins from separately generated individual building blocks.[2] Multimeric proteins constitute another illustration for a perfect fit of protein faces toward each other. A prototype is hemoglobin, which is only active in its tetrameric form and even allows allosteric regulation.[3] Multienzyme complexes, such as the one responsible for fatty acid biosynthesis[4] or ATPase,[5] can be regarded as biological assembly lines, relying completely on a perfect individual recognition of matching "robot pieces". Last but not least, antibodies scan and sense the protein surface by means of their hypervariable loops. On the contrary, protein surface recognition by designed molecules remains an unsolved challenge because the instructed synthesis of molecules with a predictable pattern of solvent-exposed functional groups is still in its infancy.[6] A perfect complementarity to the complicated topology and charge distribution on a protein surface requires the development of libraries from artificial recognition motifs and their intelligent covalent combination with a predictable conformation or folding geometry. In recent years, some pioneering groups have presented simplified solutions.[7] Synthetic α-helices with regular repeats of anionic or cationic residues can be clamped together by oligomeric tweezers, which span the helix from one end to the other and form ion pairs or inclusion complexes with each single charged amino acid residue at the correct distance of the next one.[8] Several catalytically active proteins display on their surface a hydrophobic patch surrounded by positively charged amino acids. A complementary protein receptor design involves a central core unit from a hydrophobic template, such as a calixarene or a porphyrine unit, carrying pendant negatively charged arms for a lateral recognition of lysines and arginines.[9] However, these artificial receptor

(1) Stites, W. E. *Chem. Rev.* **1997**, *97*, 1233−1250.
(2) (a) Bloomer, A. C.; Champness, J. N.; Bricogne, G.; Staden, R.; Klug, A. *Nature* **1978**, *276*, 362−368. (b) Namba, K.; Stubbs, G. *Science* **1986**, *231*, 1401−1406.
(3) Baldwin, J. *Trends Biochem. Sci.* **1980**, *5*, 224−228. (b) Perutz, M. F.; Fermi, G.; Luisi, B.; Shaanan, B.; Liddington, R. C. *Acc. Chem. Res.* **1987**, *20*, 309−321.
(4) (a) Wakil, S. J.; Stoops, J. K.; Joshi, V. C. *Annu. Rev. Biochem.* **1983**, *52*, 537−579. (b) Wakil, S. J. *Biochemistry* **1989**, *28*, 4523−4530.
(5) (a) Walker, J. E. Les Prix Nobel; The Nobel Foundation: Stockholm, Sweden,1997; pp 208−234. (b) Walker, J. E. *Angew. Chem., Int. Ed.* **1998**, *37*, 2308−2319. (c) Stock, D.; Leslie, A. G. W.; Walker, J. E. *Science* **1999**, *286*, 1700−1705.
(6) (a) Cushman, M.; Kanamathareddy, S.; De Clerq, E.; Schols, D.; Goldman, M. E.; Bowen, J. A. *J. Med. Chem.* **1991**, *34*, 337−342. (b) Regan, J.; McGarry, D.; Bruno, J.; Green, D.; Newman, J.; Hsu, C. Y.; Kline, J.; Barton, J.; Travis, J.; Choi, Y. M.; Volz, F.; Pauls, H.; Harrison, R.; Zilberstein, A.; Ben-Sasson, S. A.; Chang, M. *J. Med. Chem.* **1997**, *40*, 3408−3422.
(7) For a comprehensive review about the stabilization of α-helices and β-sheets, see: Schneider, J. P.; Kelly, J. W. *Chem. Rev.* **1995**, *95*, 2169−2187.
(8) (a) Peczuh, M. W.; Hamilton, A. D.; Sanchez-Quesada, J.; Mendoza, J. D.; Haack, T.; Giralt, E. *J. Am. Chem. Soc.* **1997**, *119*, 9327−9328. (b) Tabet, M.; Labroo, V.; Sheppard, P.; Sasaki, T. *J. Am. Chem. Soc.* **1993**, *115*, 3866−3868.
(9) (a) Hamuro, Y.; Calama, M. C.; Park, H. S.; Hamilton, A. D. *Angew. Chem., Int. Ed. Engl.* **1997**, *36*, 2680−2683. (b) Park, H. S.; Lin, Q.; Hamilton, A. D. *J. Am. Chem. Soc.* **1999**, *121*, 8−13. (c) Lin, Q.; Park, H. S.; Hamuro, Y.; Lee, C. S.; Hamilton, A. D. *Biopolymers* **1998**, *47*, 285−297.

10.1021/ja045785d CCC: $30.25

molecules require a very demanding multistep synthetic protocol or tedious separation procedures since they must cover with one molecule a large nonsymmetric protein surface area. A self-assembly of small receptor units within the fluidic environment of a lipid mono- or bilayer offers an enormous advantage in this respect. The synthetic effort is restricted to a single recognition unit which is brought into a well-ordered environment by self-assembly. In addition, due to the dramatic change in polarity from the aqueous to the lipid phase, the dielectric constant in the critical recognition zone close to the lipid surface is dramatically lowered, with the consequence of drastically enforced electrostatic and hydrogen bond interactions (by a factor of $\sim 10^6$).[10] Several groups have used these favorable circumstances for peptide and protein recognition at mono- and bilayers. Equimolar mixed monolayers of a diglycine and a guanidinium amphiphile were shown to bind free dipeptides by a guanidinium carboxylate interaction and stable antiparallel hydrogen bonds among the peptide chains.[11] Size matching of amino acid residues in host and guest leads to a certain sequence selectivity for aliphatic peptides. Kunitake et al. also used a synthetic bilayer evenly covered with phosphate anions to bind a basic protein in water at millimolar concentrations.[12] This interaction blocked the active site of an endonuclease, which was afterward not able any more to cleave DNA as efficiently as in its free state (supramolecular holoenzyme). In this case, the surface of their bilayer membrane was covered with phosphate ions for a nonspecific electrostatic attraction of the positively charged protein surface. Matile et al. recently reported a possible explanation for the cell-permeating activity of arginine-rich protein transduction domains, which have received considerable attention because they transport anionic substrates across membranes. Extensive phase-transfer experiments with liquid and bilayer membranes support their concept of "counteranion scavenging".[13] In an alternative approach, Koh et al. immobilized BSA on gold surfaces by noncovalent interaction with calix[4]arene derivatives carrying carboxylate groups at their upper rims.[14] The new SAMs were examined with SPR and showed a higher BSA concentration on those surfaces adorned with carboxylates rather than those with ester groups.

We describe in this account how lipid monolayers can be doped with a small amount of artificial receptor units which self-assemble over complementary protein surfaces and lead to large monolayer expansions. It is a state-of-the-art process to reconstitute natural receptors in lipid bilayers[15] or to bind tagged proteins to lipid monolayers.[16] Very few reports, however, have appeared about artificial receptors in membrane models,[17] and virtually nothing is known about a biomimetic version of the polyvalent self-assembly of those systems.[18] In the last part of this account, we will detail how different proteins can be detected at 10^{-8} M concentrations by using fingerprints from film balance experiments with varying simple receptor units embedded in monolayers at the air−water interface.

Table 1. Association Constants and Free Binding Energies for the Complexes between Calix[4]arene Tetraphosphonate **1** and Basic Amino Acids[a]

entry	guest	K_a (M^{-1})	ΔG (kcal/mol)	stoichiometry
1	Ts−Arg−OMe	1×10^4 (±12%)	−5.9	1:1
2	H−Arg−OH	8×10^2 (±28%)	−4.0	1:1
3	Ac−Lys−OMe	7×10^2 (±42%)	−3.9	1:1
4	H−Lys−OH	3×10^3 (±25%)	−4.8	1:1
5	Ac−Val−OMe	<10	<1.0	
6	Ac−Ser−OMe	<10	<1.0	

[a] Arginine and lysine were examined in their free and N/C-protected form in methanol by NMR titrations at ambient temperature (20 °C).

Discussion

Solution Studies: Selective Binding of Basic Amino Acids by Calixarene Tetraphosphonate 1. We have recently described a calixarene tetraphosphonate which forms highly stable molecular capsules with complementary cationic half-spheres in polar solvents.[19] When we examined its potential to bind simple cationic ligands, such as basic amino acids and peptides, we discovered a high affinity in methanol for arginine and lysine derivatives. We first carried out binding experiments of single calixarene tetraphosphonates in free solution with various arginine and lysine derivatives and then moved on to investigations in a monolayer.[20] The related tetrasulfonato calix[*n*]arenes have recently been discovered to bind amino acids by electrostatic and π-cation interactions.[21] They also block chloride ion channels and act antithrombotic as well as antiviral, without any considerable haemolytic or immunogenic properties.[22]

The regular arrangement of four phosphonate anions in a square strongly suggests that monocationic guests which fit inside will be drawn into the center of negative charge density right in the middle of the four functionalities. This binding mode might be reinforced by $NH^+\cdots{}^-O{=}P$ hydrogen bonds and by the electron-rich interior of the calixarene, whose benzene rings on the concave inner side are well suited for π-cation interactions. We carried out NMR titrations in methanol and calculated the K_a values from the resulting binding isotherms by nonlinear regression methods.[23] The results are summarized in Table 1.

Guanidinium ions and alkylammonium ions are both bound very well by a combination of salt bridges and hydrogen bonds. Whereas the guanidinium cation fits snugly into the plane between all four $-O-P{=}O$ moieties, with all of its $NH^{\delta+}$ protons engaged in hydrogen bonds, lysine's ϵ-NH_3^+ functionality is accommodated in a chelate arrangement between two

(10) For an overview and first examples, see: Ariga, K.; Kunitake, T. *Acc. Chem. Res.* **1998**, *31*, 371−378.
(11) (a) Cha, X.; Ariga, K.; Onda, M.; Kunitake, T. *J. Am. Chem. Soc.* **1995**, *117*, 11833. (b) Ariga, K.; Kamino, A.; Cha, X.; Kunitake, T. *Langmuir* **1999**, *15*, 3875−3885.
(12) Kimzuka, N.; Baba, A.; Kunitake, T. *J. Am. Chem. Soc.* **2001**, *123*, 1764−1765.
(13) Sakai, N.; Matile, S. *J. Am. Chem. Soc.* **2003**, *125*, 14348−14356.
(14) Lee, M.; An, W. G.; Kim, J.-H.; Choi, H.-J.; Kim, S.-H.; Han, M.-H.; Koh, K. *Mater. Sci. Eng., C* **2004**, *24*, 123−126.
(15) Zamah, A. M.; Delahunty, M.; Luttrell, L. M.; Louis, M.; Lefkowitz, R. J. *J. Biol. Chem.* **2002**, *277*, 31249−31256.
(16) Schmitt, L.; Bohanon, T. M.; Denzinger, S.; Ringsdorf, H.; Tampé, R. *Angew. Chem., Int. Ed. Engl.* **1996**, *35*, 317−320.
(17) For embedded isolated artificial receptors in lipid layers, see: (a) Kolusheva, S.; Shahal, T.; Jelinek, R. *J. Am. Chem. Soc.* **2000**, *122*, 776−780. (b) Sasaki, D. Y.; Waggoner, T. A.; Last, J. A.; Alam, T. M. *Langmuir* **2002**, *18*, 3714. (c) Lahiri, J.; Fate, G. D.; Ungashe, S. B.; Groves, J. T. *J. Am. Chem. Soc.* **1996**, *118*, 2347.
(18) For a self-assembled receptor at the air−water interface, see: Higuchi, M.; Koga, T.; Taguchi, K.; Kinoshita, T. *Langmuir* **2002**, *18*, 813−818.
(19) Zadmard, R.; Schrader, T.; Grawe, T.; Kraft, A. *Org. Lett.* **2002**, *4*, 1687−1690.
(20) The solution studies offer the advantage of a precise determination of association constants, stoichiometries, and complex geometries. This characterization becomes much more difficult in a lipid monolayer.
(21) (a) Sansone, F.; Barboso, F.; Casnati, A.; Sciotto, D.; Ungaro, R. *Tetrahedron Lett.* **1999**, *40*, 4741−4744. (b) Da Silva, E.; Coleman, A. W. *Tetrahedron* **2003**, *59*, 7357−7364.
(22) (a) Gansey, M. H. B. G.; de Haan, A. S.; Bos, E. S.; Verboom, W.; Reinhoudt, D. N. *Bioconjugate Chem.* **1999**, *10*, 613−623. (b) Da Silva, E.; Shahgaldian, P.; Coleman, A. W. *Int. J. Pharm.* **2004**, *273*, 57−62.

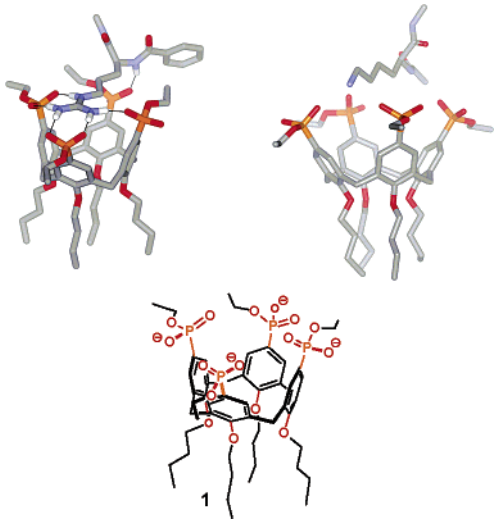

Figure 1. Optimized complex structure between N/C-protected arginine, N/C-protected lysine, and calixarene tetraphosphonate **1**. After energy minimization, a Monte Carlo simulation was carried out in water (MacroModel 7.0, 3000 steps).

phosphonates, with its peptidic amide reaching over to one of the other phosphonates at the calixarene's upper rim. Force-field calculations, including Monte Carlo conformational searches, reach intriguing complex geometries which are in accord with all spectroscopic information (Figure 1).[24] These binding patterns lead to a high affinity for the side chain of arginine (10^4 M^{-1})[25] and one order of magnitude lower for lysine. Even in the free zwitterionic form with repulsive carboxylates, binding constants in methanol are still in the order of 10^3 M^{-1} (Figure 1). It must be emphasized that the complexes of calixarene tetraphosphonate **1** with arginine and lysine derivatives cannot be compared to those described earlier for calixarene tetrasulfonates.[26] Whereas large methylene upfield shifts indicate that the δ-guanidinium and ϵ-ammonium groups penetrate deeply into the cavity of the calixarene sulfonate, only small shifts are produced with the phosphonate pendant. Obviously, the nature of intermolecular attraction is, in our case, mainly electrostatic, perhaps because of the more basic phosphonate anions, which are known to form strong chelate complexes with organic cations.[27]

No other amino acid side chain produced complexation-induced shifts in NMR titrations ($\Delta\delta_{max}$ < 0.02 ppm).[28] Thus, the calixarene tetraphosphonate can be considered to be a specific receptor molecule for basic amino acid side chains, with a preference for arginine.

Incorporation of Tetraphosphonate Calixarene 1 into a Lipid Layer: Recognition of Basic Amino Acids, Peptides, and Proteins by Multipoint Interactions. Since the tetraanionic receptor molecule has an amphiphilic structure with polar headgroups at the upper rim and nonpolar butoxy-tails at the lower rim, an incorporation into lipid monolayers seemed to be quite feasible. As explained above, the dielectric constant of the water subphase near the lipid monolayer is much lower than usual;[29] we therefore envisaged that noncovalent interactions based on ion pairing would be strengthened in such an environment, leading to efficient and hopefully specific molecular recognition of cationic analytes at the air−water interface. This concept, indeed, turned out to be very practicable and valuable.

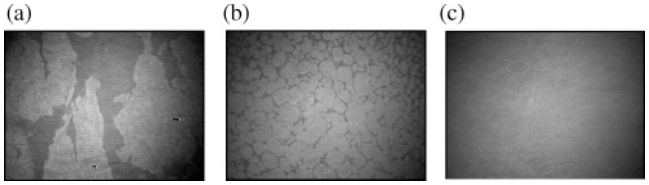

Figure 2. BAM pictures taken (a) directly, (b) 5 min, (c) 15 min after addition of tetraphosphonate **1** to the stearic acid monolayer; initially appearing patches of receptor molecule domains dissolve readily and finally produce a smooth surface of evenly distributed calixarenes in the monolayer.

When increasing concentrations of the tetraphosphonate were added to a stearic acid monolayer on water, increasing amounts of receptor molecule were indeed incorporated in the monolayer, indicated by regular shifts in the pressure/area diagram.[30] Intact patches of receptor molecules immobilized in the monolayer could be visualized by the BAM technique (Brewster angle microscope, Figure 2) directly after injection;[31] however, after a few seconds, the BAM screen turned completely smooth again, demonstrating an even distribution among the surrounding excess lipid molecules (mutual repulsion of the negatively charged phosphonate anions of vicinal receptor molecules, later stabilized by hydrogen bonds to the surrounding carboxylic acid hydroxyls).

Subsequent injection of cationic analytes (e.g., basic amino acids) into the aqueous subphase produced moderate, but distinct, additional expansions of the pressure/area diagrams. In each case, no interaction was observed between any of the ligands and the stearic acid monolayer alone. Even more efficient was the stepwise formation of the lipid/receptor monolayer over a homogeneous subphase of known analyte concentration (Figure 3). The binding mode of the monocationic guests identified in the solution studies provides a good explanation for the moderate effects in the film balance; effective complexation does not require more space, but occurs mainly beneath the cavity of the calixarene tetraphosphonate (vide supra). We believe that our calixarenes adopt a parallel orientation inside the monolayer originating from their strongly amphiphilic nature, without showing any self-association at the concentrations involved in the above-mentioned experiments (NMR dilution). The alternative perpendicular orientation requires more space, as was shown by others, and results in a compression plateau near 28 mN/m. The absence of such a compression plateau in the π-A diagram strongly indicates that

(23) (a) Schneider, H. J.; Kramer, R.; Simova, S.; Schneider, U. *J. Am. Chem. Soc.* **1988**, *110*, 6442. (b) Wilcox, C. S. In *Frontiers in Supramolecular Chemistry*; Schneider, H. J., Ed.; Verlag Chemie: Weinheim, Germany, 1991; p 123.
(24) *MacroModel 7.0*; Schrödinger Inc. Force-field: Amber*, water, 3000 steps.
(25) In fact, this K_a value places it above all other bisphosphonates described earlier as arginine receptors.
(26) (a) Selkti, N. M.; Coleman, A. W.; Nicolis, I.; Douteau-Guével, N.; Villain, F.; Tomas, A.; De Rango, C. *Chem. Commun.* **2000**, 161. (b) Douteau-Guével, N.; Perret, F.; Coleman, A. W.; Morel, J.-P.; Morel-Desrosiers, N. *J. Chem. Soc., Perkin Trans. 2* **2002**, 524−532.
(27) (a) Schrader, T. *Chem.−Eur. J.* **1997**, *3*, 1537. (b) Rensing, S.; Springer, A.; Grawe, T.; Schrader, T. *J. Org. Chem.* **2001**, *66*, 5814−5821. (c) Rensing, S.; Schrader, T. *Org. Lett.* **2002**, *4*, 2161−2164.
(28) For related work, see: Schrader, T. *Chem.−Eur. J.* **1997**, *3*, 1537.
(29) Sakurai, M.; Tamagawa, H.; Inoue, Y.; Ariga, K.; Kunitake, T. *J. Phys. Chem. B* **1997**, *101*, 4810−4817.
(30) Quite recently, calixarene 1,3-bisphosphonates with alternating hydrophilic and hydrophobic groups have been prepared and integrated into monolayers entirely consisting of two-dimensional condensed-phase domains: Vollhardt, D.; Gloede, J.; Weidemann, G.; Rudert, R. *Langmuir* **2003**, *19*, 4228−4234.
(31) Hönig, D.; Möbius, D. *J. Phys. Chem.* **1991**, *95*, 4590.

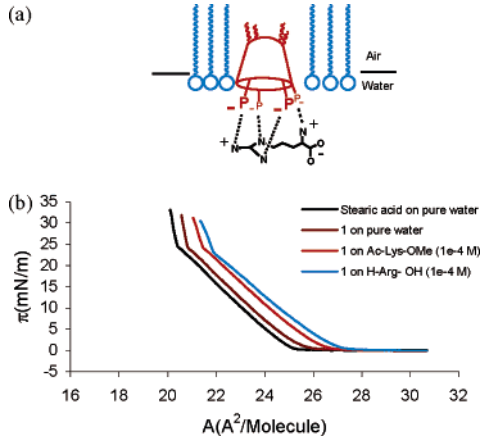

Figure 3. (a) Schematic representation of the calixarene in the monolayer recognizing an arginine guest in the subphase. (b) Pressure/area isotherms for the embedding of receptor **1** (0.13 equiv) into a stearic acid monolayer on the Langmuir film balance, followed by molecular recognition of N/C-protected arginine and lysine (both 10^{-4} M). The experimental deviations between 3 and 5 independent experiments were in the range of 0.1−0.2 A^2.

our calixarene amphiphiles are oriented in the desired parallel fashion inside the monolayer.[32]

Specific and efficient biological recognition on cell surfaces usually relies on multipoint binding. We tried to imitate this process by offering analytes in the subphase which require several receptor molecules for a double or triple recognition event. Even in the highly compressed superliquid phase (SL) of a monolayer, the embedded receptor molecules can move freely around into all directions, facilitating an automatic self-assembly over polytopic guests in the subphase.[33] For a straightforward test, we used free mono-, di-, and triarginine and were surprised. From the monopeptide over the di- to the tripeptide, remarkable expansions in the pressure/area diagram were produced, confirming beautifully the hypothesis outlined above. Even at 10^{-7} M concentrations, triarginine could be easily detected in water even if the amount of embedded receptor molecule did not surpass 0.13 equiv (Figure 4).

As stated in the Introduction, Kunitake et al. recently described elegant mixed monolayers with sequence-selectivity for dipeptides, albeit at millimolar concentrations.[11] By rational design, the spatial disposition of sterically demanding amino acid side chains in their regular arrangement inside the monolayer confined the space for bound analytes and led to a remarkable sequence-selectivity for dipeptidic guests with a free carboxy terminus. Again, single hydrogen bonds and salt bridges were dramatically enforced by the altered microenvironment at the air−water interface. In our case, an isolated calixarene receptor molecule is embedded in the monolayer with approximately 200 stearic acid molecules surrounding it. To exert strong attraction on arginine or lysine-rich peptides or proteins, several of these receptor molecules must move through the monolayer and self-assemble on top of the protein surface so that they can each bind another cationic amino acid side chain (Figure 5).

The next step was the transition to larger peptides and proteins. If proteins carry a high number of arginines or to a

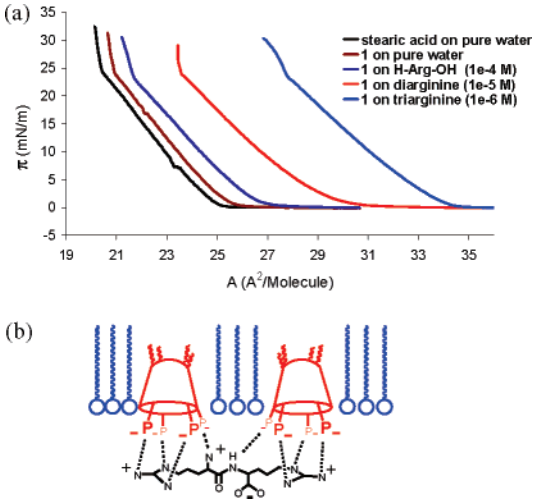

Figure 4. (a) Pressure/area isotherms for arginine (10^{-4} M), diarginine (10^{-5} M), and triarginine (10^{-6} M) on the Langmuir film balance. Receptor **1** (0.13 equiv) was embedded in the stearic acid monolayer. Note the drastic expansions of the monolayer despite the decreasing peptide concentrations in the subphase; compared to the large observed expansion of 3.5 A^2 by diarginine at 10^{-5} M, diaspartate at the same concentration produced only a small shift of 0.8 A^2. (b) Schematic representation of the multipoint binding mode in the case of diarginine recognition by the monolayer.

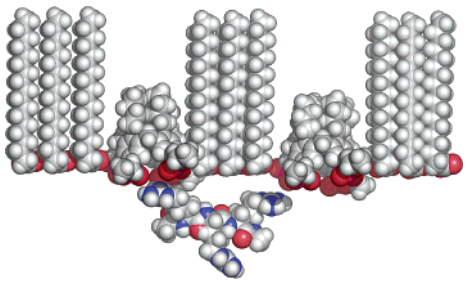

Figure 5. Graphical representation of the binding mode at the lipid monolayer; 400 stearic acid molecules surround two embedded calixarenes, both oriented with their polar headgroups into the aqueous subphase. A diarginine fragment within the triarginine guest approaches the monolayer from beneath and draws two tetraphosphonates into the correct position to interact with both guanidinium functionalities in a double chelate arrangement (two-point binding mode). In the next step, the third guanidinium cation can pull a third calixarene from behind and form the third binding site.

lesser extent also lysines on their surfaces, they should, in principle, also be able to exert multipoint binding by self-assembly of the immobilized arginine binders inside the monolayer (Figure 6a). Remarkably, the lysine-rich fraction of histone 1b, as well as the arginine-rich cytochrome *c*, furnished pronounced shifts in their respective pressure/area diagrams, even at the nanomolar level (10^{-9} M). The corresponding binding energies can compete with those gained in the most efficient protein−protein interactions, which are still effective at exactly these low concentrations.[34] More importantly, a broad variation of the salt concentration between 0.5 and 150 mM did not alter the observed increase in surface area. Similarly, the pressure/area diagrams are roughly insensitive toward a variation of the HEPES buffer concentration from 0.5 to 50 mM.[35] Proteins with IEPs clearly below 7.0 might also bind to the monolayer if a spatial separation of basic and acidic amino

(32) Liu, F.; Lu, G.-Y.; He, W.-J.; Liu, M.-H.; Zhu, L.-G.; Wu, H.-M. *New J. Chem.* **2002**, *26*, 601−606.
(33) Ulman, A. *An Introduction to Ultrathin Organic Films from Langmuir−Blodgett to Self-assembly*; Academic Press: New York, 1991.
(34) From a 10^{-8} M equimolar aqueous solution of the histone protein with the calixarene host, we obtained a clean ESI-MS spectrum. It featured prominent molecular ion peaks for the 1:1, 1:2, and 1:3 complex, with the highest intensity residing in the 1:2 peaks.

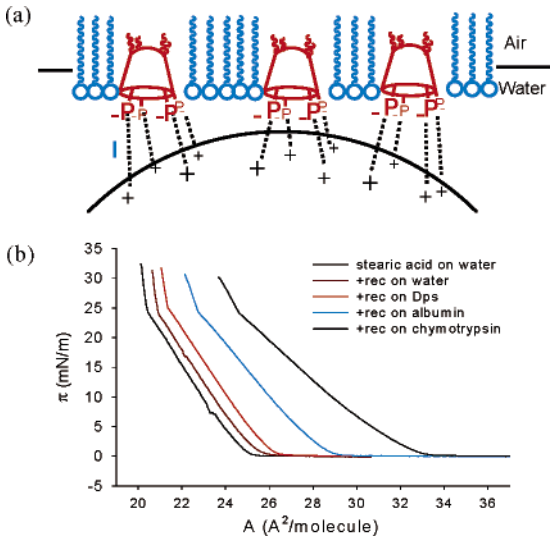

Figure 6. (a) Proposed binding mode of the embedded calixarene tetraphosphonate **1** with basic proteins in the aqueous subphase, explaining large p/A shifts only at high pI values. Interaction I: protein−NH_3^+···O_2-(RO)P^-−host. (b) Langmuir isotherms obtained from 0.13 equiv of calix-[4]arene tetraphosphonate **1** incorporated into a stearic acid monolayer at the air−water interface, over protein solutions of ∼10^{-8} M. Note the strong increase in p/A with increasing protein basicity (i.e., increasing pI).

acid residues occurred on the protein surface, leading to cationic and anionic domains. This could be proven by the effective interaction with BSA (IEP 6.0); this ubiquitous protein has a barrel-shaped overall structure with high concentrations of aspartates and glutamates on the lids, whereas the walls around their central seam are mainly covered with arginines and lysines.[36] Proteins with neutral surfaces should bind much more weakly to the calixarene receptor in the monolayer. Indeed, the Dps dodecamer[37] and an acyl carrier protein displayed only moderate shifts in the pressure/area diagram. For a better comparison, we examined all proteins at 10^{-8} M concentration and plotted the resulting isotherms in one diagram (Figure 6b).[38] Under these circumstances, most proteins do not interact with the stearic acid monolayer.[39] Weak to moderate effects are produced with acidic to essentially neutral proteins, such as ferritin and the Dps dodecamer (+1−2 A^2), whereas proteins with basic domains, such as albumin and thrombin, are more efficient (+2−3 A^2). The largest shifts, however, are found with basic proteins, such as histone H1 and chymotrypsin, whose pI surpasses 7 (+5−6 A^2). All examined proteins are listed in Table 2. An almost linear correlation combines the area increase in the monolayer ΔA_{rec} with the pI values of the respective proteins. Our simple model system can thus be regarded as an artificial imitation of the efficient and selective binding of certain proteins by multipoint recognition on cell surfaces.

Table 2. Basic, Neutral, and Acidic Proteins Recognized by Calixarene Tetraphosphonate **1** on the Langmuir Film Balance: Dependence of the Area Increase ΔA on the IEP Values at Concentrations around 10^{-8} M, Corrected for Their Individual Surface Areas

protein	c_{cor}	ΔA_{matrix}	ΔA_{rec}		MW	surface
(10^{-8} M)	(M)[a]	(A^2)[b]	(A^2)[c]	pI	(kDa)	(kA^2)[d]
histone H1	4×10^{-9}	0	5	10.4	7.7	4.3
cytochrome *c*	6×10^{-9}	0	5	9.5	12.3	6.3
proteinase K	10^{-8}	1	6	8.1	38.4	11.0
chymotrypsin	10^{-8}	1	5	8.0	28.2	11.2
thrombin	10^{-9}	1	2	7.5	32.0	15.5
albumin	4×10^{-9}	1	2	6.0	86.3	37.0
Dps (dodecamer)	7×10^{-9}	1	1	5.9	190.0	75.0
ferritin	10^{-8}	1	2	5.5	455.3	175.5
acyl carrier protein	10^{-8}	1	1	4.2	8.4	4.7
DNA (36mer)	10^{-8}	0	0	1.8	23.7	

[a] $c_{cor} = c_{exp} \times \text{surface}_{prot}/10\ kA^2$. [b] Interaction with stearic acid alone. [c] Additional interaction with the embedded receptor. [d] Connolly surface.

Host Specificity. Several groups utilized unspecific electrostatic attraction for a tight binding of oppositely charged proteins to mono- or bilayers.[12] Many chromatographic protein purification methods also rely on such unspecific binding events. It could be argued that rather than multiplying cooperative single recognition events, our high number of phosphonate anions would simply attract basic proteins by such an unspecific Coulomb interaction, although certainly in our case, only 3% of the monolayer contains the receptor structure.[40] For a direct proof, we embedded a number of related anionic amphiphiles in the same stearic acid monolayer and observed almost no effects (Figure 7). Even a xylylene bisphosphonate, which is, in free solution, moderately selective for basic amino acids, produced only very small shifts (∼0.5 A^2). With monophosphonate **1b** as well as with monosulfonate SDS **1c**, no or negligible shifts were found (0−0.5 A^2). Hence, it seems fair to say that multipoint binding of complementarily charged proteins has been demonstrated at the air−water interface, imitating the natural prototype.

From all of the above-mentioned collected experimental data, we infer the following tentative mechanism of peptide and protein binding by the monolayer (Figure 8). As guest molecules are subinjected into the aqueous phase, they are bound by solvated receptor molecules close to the monolayer. The host molecules' negative charges become, in part, neutralized, and their lipophilicity increases. This, in turn, leads to reincorporation of the whole complex into the monolayer. Thus, large amounts of receptor molecules, which are formerly dissolved in the aqueous subphase, migrate back into the monolayer as soon as they become complexed on the surface of a basic peptide or protein. Experimental evidence for this comes from the relatively small, but proportionally growing, area increase following the addition of the receptor, as opposed to the enormous expansions following the subinjection of protein

(35) In high excess, NaCl and HEPES themselves interact with the receptor molecule and are less pronounced with the stearic acid monolayer; however, the large additional increase with NaCl, due to the specific calixarene protein interaction, remains constant throughout the entire concentration range: (a) Shahgaldian, P.; Coleman, A. W. *Langmuir* **2001**, *17*, 6851−6854. (b) Houel, E.; Lazar, A.; Da Silva, E.; Coleman, A. W.; Solovyov, A.; Cherenok, S.; Kalchenko, V. I. *Langmuir* **2002**, *18*, 1374−1379. (c) Da Silva, E.; Nouar, F.; Coleman, A. W.; Rather, B.; Zaworotko, M. J. *J. Inclusion Phenom. Macrocycl. Chem.* **2003**, *46*, 161−166.

(36) (a) Carter, D. C.; He, X. M.; Munson, S. H.; Twigg, P. D.; Gernert, K. M.; Broom, M. B.; Miller, T. Y. *Science* **1989**, *244*, 1195−1198. (b) Carter, D. C.; Ho, J. X. *Adv. Protein Chem.* **1994**, *45*, 153−203.

(37) Dps is DNA protecting protein of starving bacteria.

(38) To be able to compare the absolute effects of proteins of different size, we multiplied their concentrations with their relative surface areas. As reference with a medium value, we arbitrarily chose the ferritin monomer, which has a surface area of 10 kA^2 (ferritin is composed of 24 identical subunits, each of which has a comparable size to the other monomeric basic proteins).

(39) BSA is a notable exception; even at 10^{-9} M, a strong interaction with stearic acid alone was found in the film balance experiments, leading to a beginning destruction of the monolayer at 10^{-8} M. This is clearly related to what BSA does in nature: it binds to fatty acids which have been released to the blood stream and leads to a 1000-fold increase in their solubility. Apart from BSA, thrombin, and to a small extent ferritine, the dodecamer and chymotrypsin also interact with the stearic acid monolayer.

(40) With 0.13 equiv × 210 A^2 (calixarene surface area) = +27.3 A^2 theoretical area increase, +0.8 A^2 observed area increase ∼3%.

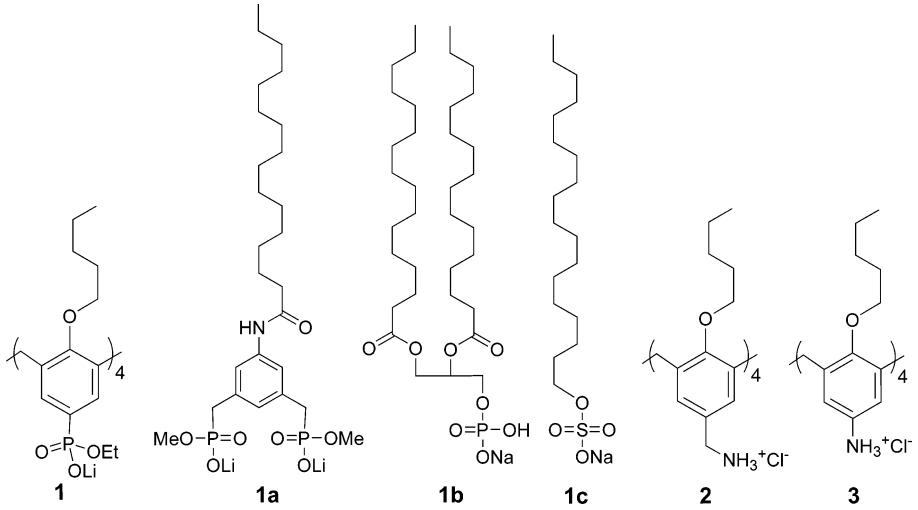

Figure 7. Host structures of all anionic and cationic amphiphiles embedded in a stearic acid monolayer, over $10^{-7}-10^{-10}$ M protein solutions: **1** calixarene tetraphosphonate, **1a** *m*-xylylene bisphosphonate, **1b** phosphoglyceride, **1c** sodium dodecyl sulfate, **2** tetrabenzylammonium calixarene, and **3** tetraanilinium calixarene.

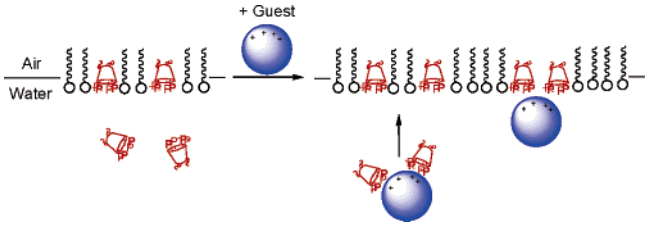

Figure 8. Model rationale to explain the large π-A shifts in the film balance experiments.

guests. Since all of these proteins are highly polar and absolutely not amphiphilic, the large p/A shifts cannot be explained with incorporation of pure protein material into the monolayer; it would simply be destroyed, as can be observed in the BAM picture. The smooth extended surface must originate from reintegration of substantial amounts of the amphiphilic receptor molecules, triggered by complex formation with the proteins. As calculated above, only a small fraction of calixarene tetraphosphonates remains in the monolayer, ~97% are dissolved in the aqueous subphase. Especially small to medium size proteins with compact basic domains, such as the histone, chymotrypsin, and cyt *c*, can easily accommodate several calixarenes in parallel orientation on their surface, which will lead to a partial charge neutralization and render the whole protein−calixarene complex amphiphilic. Eventually, this superamphiphile is reintegrated into the monolayer, leading to the remarkable expansions. It might be argued that very large proteins and even larger more polar guests, such as nucleic acids, might cause an opposite effect; after tight binding to several calixarenes, the large polar guest might pull the receptor molecules out altogether, thus leaving behind a contracted monolayer with smaller area. In these cases, the complex would significantly weaken the amphiphilic character of the calixarene, but not lower the polarity of the guest. This is exactly the case when highly charged phosphate-containing guests are complexed by tetraanilinium halfsphere **3** (Table 4). In all cases, a negative p/A effect is observed, attributed to receptor molecules being pulled out of the monolayer after binding to ATP, DNA, or even a strongly acidic protein (ACP, pI 4.2). Therefore, we conclude that in addition to the overall pK_a (pI) of the guest, its sheer size also determines the degree of monolayer expansion or contraction.

Table 3. Basic, Neutral, and Acidic Proteins Recognized by Tetrabenzylammonium Calixarene **2** on the Langmuir Film Balance: Dependence of the Area Increase ΔA on the pI Values at Concentrations around 10^{-8} M

host	subphase (M)	pI	ΔA (Å^2)	MW (kDa)
Bzlam. **2**	water		0.0 (7.2)	MW [kDa]
Bzlam. **2**	histone H1 (10^{-8})	10.4	0.8 (8.0)	7.7
Bzlam. **2**	cytochrome *c* (10^{-8})	9.5	1.4 (8.6)	12.3
Bzlam. **2**	thrombin (10^{-8})	7.5	2.0 (9.2)	32.0
Bzlam. **2**	albumin (10^{-8})	6.0	2.8 (10.0)	86.3
Bzlam. **2**	ACP (10^{-8})	4.2	4.0 (11.2)	8.4

Table 4. Basic, Neutral, and Acidic Proteins as Well as Biologically Relevant Oligophosphates Recognized by Tetraanilinium Calixarene **3** on the Langmuir Film Balance: Dependence of the Area Increase ΔA on the pI Values at Concentrations around 10^{-8} M (DNA = 36mer)[a]

entry	host	subphase (M)	pI	ΔA (Å^2)	MW (kDa)
1	anil **3**	water		0 (8.0)	
2	anil **3**	ATP (10^{-4})	1.8	−2 (6.0)	0.6
3	anil **3**	ATP (10^{-6})	1.8	−2 (6)	0.6
4	anil **3**	ATP (10^{-8})	1.8	−1.2 (6.8)	0.6
5	anil **3**	NADP (10^{-8})	1.8	−2 (6)	0.7
6	anil **3**	DNA (1.6×10^{-7})	1.8	−2.5 (5.5)	23.7
7	anil **3**	ACP (10^{-8})	4.2	−1 (7)	8.4
8	anil **3**	ferritin (10^{-8})	5.5	plateau	455.3
9	anil **3**	Dps (10^{-9})	5.9	plateau	190.0
10	anil **3**	albumin (10^{-8})	6.0	1 (9)	86.3
11	anil **3**	thrombin (10^{-9})	7.5	1 (9)	32.0
12	anil **3**	cytochrome *c* (10^{-8})	9.5	3 (11)	12.3
13	anil **3**	histone H1 (10^{-8})	10.4	5 (13)	7.7

[a] ACP = acyl carrier protein; NADP = nicotinamide adenine dinucleotide phosphate.

Incorporation of Benzylammonium Calixarene 2 into a Lipid Monolayer: Recognition of Acidic Proteins. In extension of the concept, we next shifted our attention toward the opposite case, that is, the recognition of acidic proteins by cationic amphiphiles embedded in the monolayer. To this end, we incorporated the calix[4]arene derivative **2** with four pendant benzylammonium groups at the upper rim into the stearic acid monolayer.[41] Due to its lower polarity, a large p/A shift of ~7 Å^2 occurred, corresponding to a high percentage (~30% of the

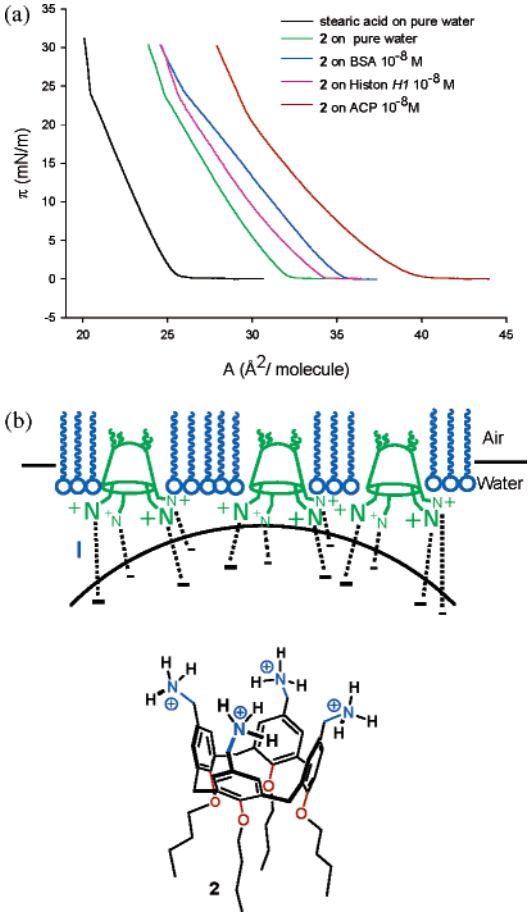

Figure 9. (a) Langmuir isotherms obtained from 0.13 equiv of benzylammonium calixarene **2** incorporated into a stearic acid monolayer at the air−water interface, over protein solutions at 10^{-8} M. Note the strong increase in p/A with increasing protein acidity (i.e., dropping pI). (b) Proposed binding mode of the embedded benzylammonium calixarene halfsphere **2** with basic and acidic proteins in the aqueous subphase, explaining large p/A shifts only at low pI values. Interaction I: protein−CO_2^-···NH_3^+−CH_2−host.

offered 0.13 equiv) of receptor molecules present in the monolayer (compared to that of the tetraphosphonate, 0.8 A^2, ∼3% of the offered 0.13 equiv). Subsequent subinjection of histone H1 (pI = 10.4) produced only a negligible additional shift of 0.8 A^2. However, as the pI of the investigated proteins decreased, the monolayer expansion strongly increased, reaching an additional 4 A^2 for the acyl carrier protein (pI = 4, Table 3). In each case, no measurable interaction occurred between the protein and the stearic acid monolayer alone, confirming a specific effect of the embedded cationic calixarene on the dissolved guest in the subphase. Thus, a complementary system can be established, which is selective for acidic proteins at a concentration of 10^{-8} M (Figure 9). It could even be argued that with our doped monolayers, we can indirectly measure the pI of dissolved proteins at a constant given concentration.

To our surprise, NMR titrations of diaspartate dicarboxylate with the tetracationic receptor **2** or **3** did not furnish appreciable complexation-induced shifts, even at millimolar concentrations in methanol. Only in DMSO could a distinct interaction be observed, leading to an association constant of ∼10 000 M^{-1}.

(41) Diaminocalix[4]arenes were recently shown to interact with nucleotides at the air−water interface: Liu, F.; Lu, G.-Y.; He, W.-J.; Liu, M. H.; Zhu, L.-G. *Thin Solid Films* **2002**, *414*, 72−77.

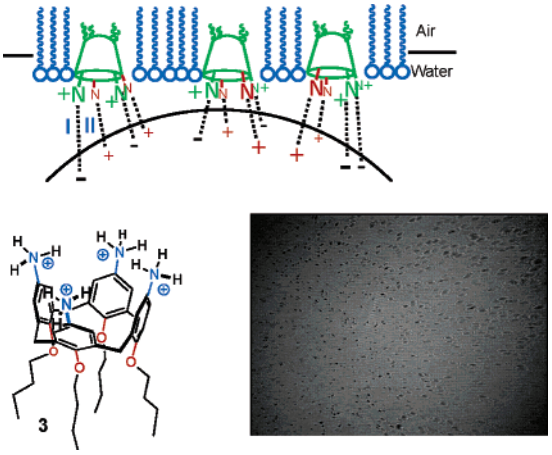

Figure 10. Proposed binding mode of the embedded anilinium calixarene halfsphere **3** with basic and acidic proteins in the aqueous subphase, explaining large p/A shifts at both low and high pI values. Interaction I: protein−NH_3^+···NH_2−host. Interaction II: protein−CO_2^-···NH_3^+−Ar−host. BAM picture: Small growing aggregates indicating the beginning destruction of the monolayer due to tight binding between very large acidic proteins (Dps/ferritin, pI 5.5−5.9, MW 190−455 kDa) and anilinium halfsphere **3** at 15−20 mN/m.

Thus, the single 1:1 interaction between aspartate residues and the calixarene tetraammonium ion is too weak to be measured by NMR in polar solution. Nevertheless, it becomes a dominant attractive force at the air−water interface, due to the lowered dielectric constant and the multiplication combined with self-assembly (cooperative effect).

Incorporation of Anilinium Calixarene 3 into a Lipid Monolayer: Recognition of All Polar Proteins. Anilinium ions are entropically favorable compared to benzylammonium ions, although their lower pK_a of ∼4.5 renders them partially deprotonated at neutral pH. We synthesized the respective calix[4]arene halfsphere **3** and found that it even more readily enters the unpolar environment of the stearic acid monolayer. A p/A expansion of 8.0 A^2 was observed, corresponding to incorporation of ∼40% of the offered 0.13 equiv of host compound. Then, we determined the pK_a values for both cationic building blocks by potentiometric titration and an analysis based on difference plots. Whereas the benzylammonium calixarene **2** shows a pronounced decrease in acidity from the first to the second protonation stage (pK_a = 10.1, 9.4, 7.9, and 3.7 ± 0.1), the pK_a values for the more acidic anilinium calixarene **3** show a relatively narrow distribution (5.2, 4.5, 4.0, and 3.5 ± 0.1).[42] In the case of anilinium derivative **3**, only a relatively small fraction of the cationic species is fully protonated at neutral pH. Both protonated NH_3^+ groups and especially free NH_2 amino groups are present in each tetraanilinium halfsphere. Indeed, this completely changes its recognition profile toward a wide range of guests varying in size, polarity, and pI.

At neutral pH, aspartate and glutamate containing small peptides are also not fully deprotonated due to their relatively high pK_a of ∼4.8. On the contrary, oligophosphate anions are permanently charged over a wide pH range (Table 4, entries 1−6; Figure 11, top). Therefore, as a model guest, we chose ATP, which carries at least three negative charges, and found a negative p/A shift of 2 A^2 with the embedded anilinium

(42) Potentiometric titrations were carried out in water/DMSO (benzylammonium) or 2:1 water/methanol (anilinium) solvent mixtures at 25 °C and an ionic strength of 0.1 M (KCl). For details of the analytical procedure, see: Kraft, A. *J. Chem. Educ.* **2003**, *80*, 554−559 and references therein.

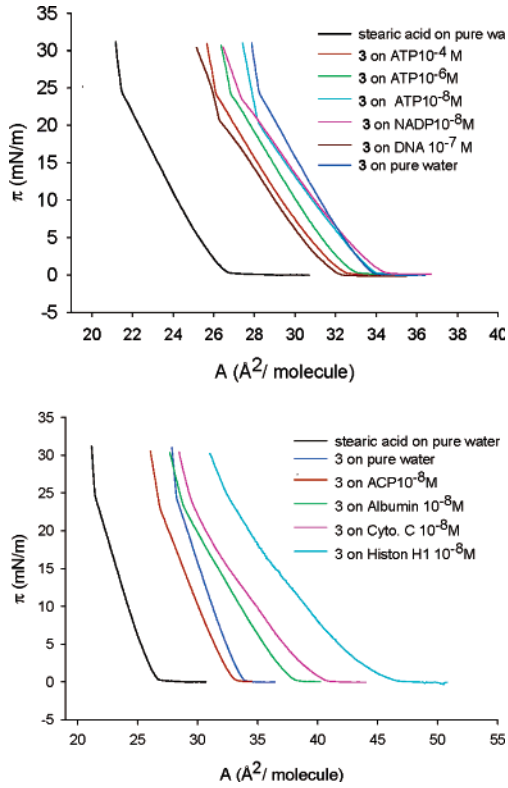

Figure 11. Pressure/area isotherms for oligophosphates (above) and proteins (below) ($\sim 10^{-8}$ M) of varying pI with the embedded anilinium halfsphere **3** (0.13 equiv) in a stearic acid monolayer. Note the strongest effects at pI values markedly above and below neutrality.

halfsphere **3**. Again, no effect was measured between ATP even at high concentrations and stearic acid alone. We explain the negative shift simply by a reversed solubility situation; the highly polar triphosphate binds to the embedded receptor amphiphile and pulls it out of the monolayer into the aqueous subphase. This interaction is so strong that even after lowering the ATP concentration by 4 orders of magnitude, the p/A shift remained still higher than 1 A^2. Quite similar effects were observed with NADP and a small DNA fragment (30 base pairs) at submicromolar concentrations. Each of these highly polar solutes draws the calixarene into the aqueous subphase.

The picture changed profoundly when we moved to protein solutions (entries 7−13; Figure 11, bottom). Large positive effects are observed, especially in the basic pI region (entries 12 and 13). As the pI approaches 7, the effects decrease considerably (entries 10 and 11). Even lower protein pI values, corresponding to acidic surfaces, lead to a destabilization of the monolayer. Thus, smaller proteins trigger a host migration into the water phase, whereas larger proteins produce a broad compression plateau, accompanied by growing black spots on the BAM screen. (Obviously, at high pressures, the formerly well-ordered monolayer breaks at the attachment points of the giant protein coils, and one layer slides on top of the other producing aggregates visible in the BAM (Figure 10).) Strong interactions with basic and acidic proteins are in good agreement with the mixture of strong hydrogen bond donor and acceptor groups at the calixarene's upper rim. Free amino functions are capable of forming ionic hydrogen bonds to arginine and lysine residues, whereas the ammonium groups will form salt bridges and ion-pair reinforced hydrogen bonds with aspartates and glutamates on the protein surface (Figure 5). Only noncharged or neutral proteins will interact weakly with this NH_2/NH_3^+ receptor chameleon.

Table 5. Basic, Neutral, and Acidic Proteins Recognized by a Combination of Calixarene Tetraphosphonate **1** (0.13 equiv) and **2** (0.13 equiv) or **3** (0.13 equiv) on the Langmuir Film Balance: Dependence of the Area Increase ΔA on the pI Values at Concentrations around 10^{-8} M

entry	receptor unit	solute	pI	ΔA (A^2)	MW (kDa)
1	**1** and **3**	water		0 (10.0)	
2	**1** and **3**	histone H1 (10^{-8})	10.4	8.7 (18.7)	7.7
3	**1** and **3**	cytochrome *c* (10^{-8})	9.5	6 (16)	12.3
4	**1** and **3**	thrombin (10^{-9})	7.5	2 (12)	32.0
5	**1** and **3**	albumin (10^{-8})	6.0	5.2 (15.2)	86.3
6	**1** and **3**	ACP (10^{-8})	4.2	3 (13.0)	8.4
7	**1** and **2**	water		0 (13.0)	
8	**1** and **2**	albumin (10^{-10})	6.0	4.2 (17.2)	86.3
9	**1** and **2**	albumin (10^{-11})	6.0	0.5 (13.5)	86.3

Incorporation of Anionic and Cationic Calixarenes into a Lipid Monolayer: Increased Selectivity and Sensitivity. Various biological examples demonstrate a cooperation between different protein domains within membranes which form an active complex by self-assembly; thus, tyrosine kinases and the regulation of fructose-1,6-diphosphate formation by phosphofructokinase both rely on a self-organization process of membrane-spanning receptor domains into catalytically active biological systems. Our above-described calixarene halfspheres represent an interesting case of a modular system whose building blocks can be readily modified by chemical synthesis with respect to their functional groups presented into the aqueous subphase. It is, in principle, conceivable that a combination of two different calix[4]arenes with opposite charges at their upper rims runs into two extremes; multiple electrostatic attraction reinforced by mutual chelation may produce molecular capsules, which will probably neither enter the monolayer because they are no longer amphiphilic nor receive any protein guests because all of their binding sites are already saturated. However, strong van der Waals interactions within the lipid layer, as well as good solvation of their polar headgroups, may also keep all of the amphiphilic calixarenes as single halfspheres perpendicularly oriented inside the fluidic monolayer, despite their opposite charges. In fact, they may even form loose clusters, with an ammonium group of one receptor molecule attracting a phosphonate group of its neighbor. Such an arrangement would then represent a superb microenvironment for a cooperative recognition of charged protein surfaces; each charged calixarene building block moves freely inside the monolayer until it is located exactly above an oppositely charged amino acid residue on the protein surface. Both potential pathways should produce such extremely different results that a simple film balance investigation should easily discern among them. In a preliminary experiment, we embedded 0.13 equiv of tetraphosphonate **1** into the stearic acid monolayer, followed by 0.13 equiv of the tetrabenzylammonium halfsphere **2** or the tetraanilinium halfsphere **3**. A large extension of the surface area was monitored, even more than a simple addition would have predicted (Table 5, entries 1 and 7). This result strongly suggests that both halfspheres are embedded inside the monolayer and even stabilize each other by Coulomb attraction. A capsule formation seems highly improbable, but cannot be excluded a priori, because the whole containers might be included inside the monolayer. It should be kept in mind that these compact structures are highly stable even in polar solvents, with K_a values

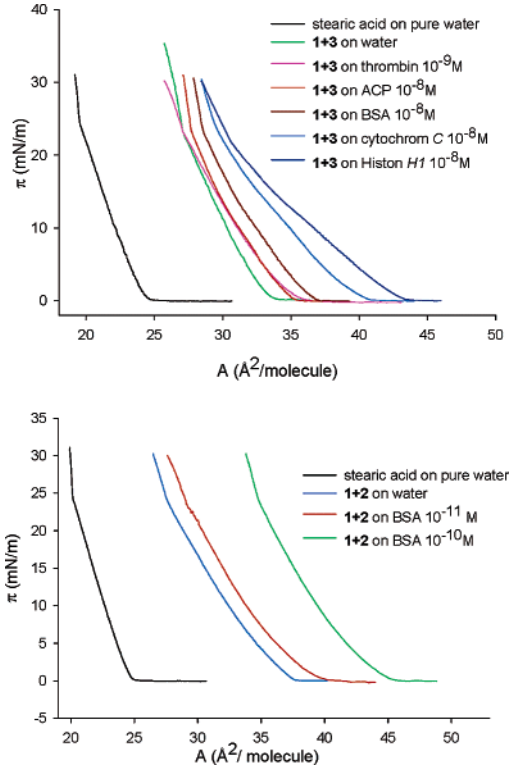

Figure 12. Top: pressure/area isotherms for proteins of varying pI (between 6 and 10.4) at 10^{-8} M with the combination of embedded phosphonate **1** and anilinium halfsphere **3** (0.13 equiv) in a stearic acid monolayer. Note the extremely large effects. Bottom: pressure/area isotherms for BSA (pI 6.0, at 10^{-10} and 10^{-11} M) with the combination of embedded phosphonate **1** and benzylammonium halfsphere **2** (0.13 equiv) in a stearic acid monolayer. Note the extremely large effects even at subnanomolar concentrations.

approaching 10^5 M^{-1} in water. However, subinjection of various proteins at 10^{-8} M produced additional large surface area expansions of up to ~9 A^2 (entries 2−6; Figure 12, top). This can only be explained if the receptor building blocks are oriented in an upright position inside the monolayer, with their cavities adorned with functional groups open to the aqueous subphase. Particularly, protein guests which possess charged domains on their solvent-exposed surfaces will be ideal binding partners, which after complexation of the calixarene anions and cations, may transport these back into the monolayer and thus lead to the large observed additional p/A effects. The BSA barrel structure is known for its dual character with three glutamate-rich domains on each face and a lysine-rich seam region. This protein can now be easily observed at subnanomolar concentrations, with a detection limit of ~10 pmol/L (entries 8 and 9; Figure 12, bottom). In summary, the cooperative combination of oppositely charged calix[4]arene halfspheres in a monolayer renders it highly sensitive for polar protein detection at the subnanomolar level.

Langmuir−Blodgett Layers: Direct Proof of Noncovalent Protein Binding to the Monolayer and Quantitative Estimation of Binding Strength. Direct proof of the noncovalent protein binding to the monolayer could be achieved for basic and neutral proteins with the Langmuir−Blodgett (LB) technique; 160 superimposed monolayers were drawn from the air−water interface doped with **1** by a conventional LB dipping procedure over a 10^{-8} M cytochrome *c* subphase. The subsequent UV spectroscopic measurement reveals the presence of

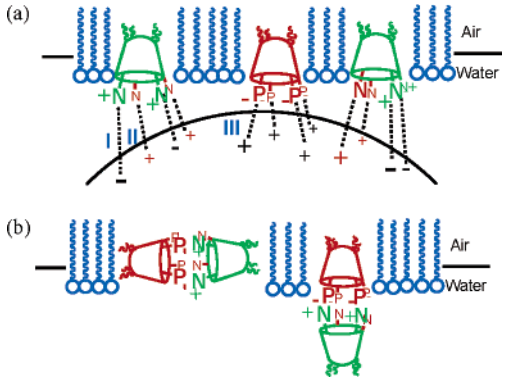

Figure 13. (a) Proposed binding mode for the combination of embedded phosphonate and ammonium calixarene halfspheres **1** and **2/3**, with proteins presenting cationic and anionic domains in the aqueous subphase. Interaction I: protein−CO_2^-···NH_3^+−Ar−host. Interaction II: protein−NH_3^+···NH_2−host. Interaction III: protein−NH_3^+···$O_2(RO)P^-$−host. (b) The second depicted alternative, capsule formation, cannot explain the observed extremely large p/A shifts at very low protein concentrations.

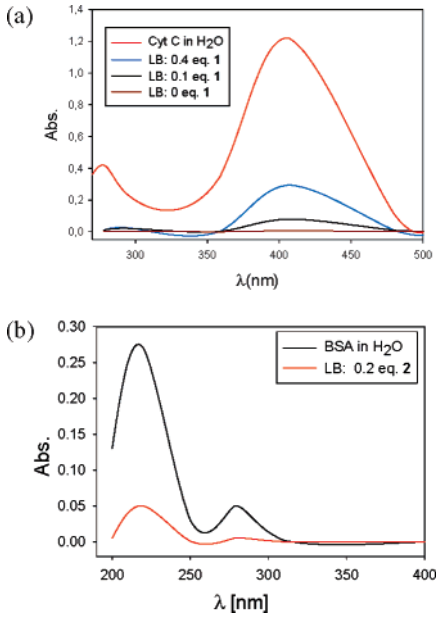

Figure 14. (a) UV−vis spectra of cytochrome *c* in water and in LB films drawn from the film balance experiments without, with 0.1, and with 0.4 equiv of embedded calixarene tetraphosphonate **1**. (b) UV−vis spectra of BSA in water and in LB films drawn from the film balance experiments with embedded benzylammonium calixarene **2**.

cytochrome *c*'s porphyrin band at 400 nm, proportional to the amount of embedded **1**, and thus provides evidence for the tight and specific protein binding. In addition, the same procedure was repeated with bovine serum albumin, an essentially neutral protein, and the benzylammonium halfsphere **2**. Again, a strong UV band developed, this time at the extinction maximum of ~250 nm, when 80 superimposed LB layers were subjected to direct UV absorption (Figure 14a,b). We also tried the same experiment on the acidic acyl carrier protein, ACP, but failed to see any additional UV absorption, even after embedding 0.4 equiv of receptor molecule **2**. The reason most likely lies in the insufficient UV absorption intensity. Even at 10^{-4} M, the aqueous free stock solution displayed only a relatively weak UV absorption. A quantitative protein detection was attempted by a variation of (a) the amount of embedded receptor molecule inside the monolayer and (b) the protein concentration in the aqueous subphase. Although a 4-fold amount (0.4 equiv) of

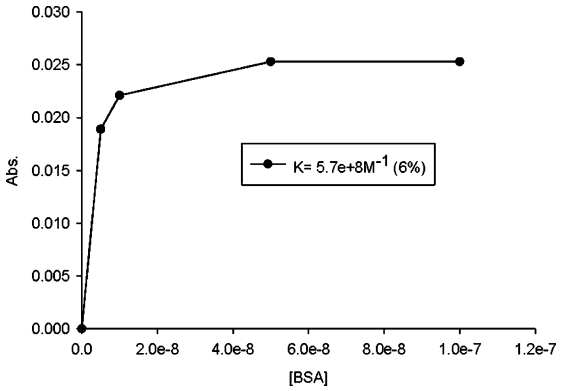

Figure 15. Dependence of the UV−vis absorbance at the extinction maximum of BSA [222 nm] in LB films drawn from doped monolayers above protein solutions with concentrations increasing from 10^{-9} to 10^{-7} M. Note the saturation above a critical value of $\sim 5 \times 10^{-9}$ M. Since the total host concentration was 7×10^{-9} M and the nonlinear regression produced an optimal fit at $\sim 2 \times 10^{-9}$ M, we infer a stoichiometry of roughly 3−4 calixarenes per BSA protein unit.[43]

benzylammonium halfsphere **2** was incorporated into the stearic acid monolayer over a 10^{-8} M BSA solution, and the resulting deposited LB multilayers looked glossy, the UV spectrum showed the same maximum extinction as before with 0.13 equiv of **2**. However, a 10-fold increase in protein concentration to 10^{-7} M BSA led to a distinct increase in signal intensity in the UV−vis spectrum. Gradually increasing protein concentrations thus furnished a calibration curve suitable for quantitative detection of the protein (Figure 15). Since at higher protein (guest) concentrations it shows saturation characteristics, nonlinear regression was applied to estimate an approximate K_a value, which was calculated at $3-5 \times 10^8$ M^{-1}, and it beautifully confirms the expected binding strength of the monolayer protein complexes. The best curve fitting suggested that a calixarene trimer or tetramer occupies the complementary area on each protein molecule, resulting in a 1:1 binding model between the self-assembled polytopic receptor-doped area of the monolayer and the lipid-exposed surface of the bound protein. This makes sense because the observed large effects at nanomolar concentrations clearly indicate that the corresponding K_d values must also be in the nanomolar range.

Protein-Specific Pattern Recognition. For many biomedical applications, a simple, versatile method is required which allows protein sensing in different biochemical environments and mixtures.[44] Among others, the facile detection of signaling proteins has become an important step in proteomics projects.[45] Especially after deciphering the human genetic code, a vast number of new protein structures will become available, with an increasing knowledge about their individual biological function due to gene mapping. In medical diagnostics, a group of lead proteins characteristic for a certain disease must be efficiently detected. Protein detectors have hitherto been based on antibody fragments,[46] monoclonal antibodies,[47] or RNA aptamers,[48] with their well-known disadvantage of chemical

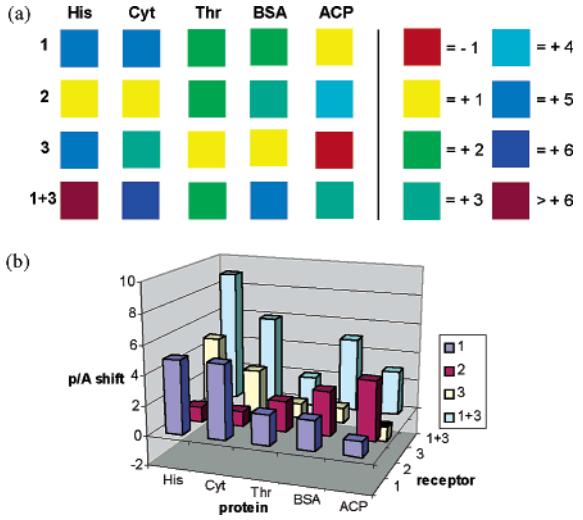

Figure 16. (a) Recognition pattern evolving from film balance experiments with five different proteins (histone H1, cytochrome *c*, thrombin, BSA, and ACP) and four different calixarene receptor cocktails (**1**, **2**, **3**, and **1**+**3**). Color coding represents p/A shifts in A^2. (b) Fingerprints of the five proteins based on the doped monolayer expansion assay. In all cases, the protein concentration was 10^{-8} M.

lability and the necessity of protein labeling. Hamilton et al. very recently presented solution arrays of fluorescent protein receptors as a straightforward answer to this problem. A library of eight tetraphenylporphyrin (TPP) derivatives functionalized with different amino acids was synthesized and separated into single components of varying total charge. These were individually incubated on a 96 well plate with a 3-fold excess of four different proteins covering the whole pI range. When irradiated with UV light, the plate showed a pattern of fluorescent and nonfluorescent wells, correlating with fluorescence quenching upon protein binding. It was argued that each column of the plate corresponded to a unique fingerprint, characteristic of the respective protein. This very promising approach has two major limitations; the tetraphenylporphyrin derivatives require a multistep synthesis or a tedious separation process which can only be carried out on a small scale; in addition, the method was carried out at 10 μM concentrations in order to ensure a *naked eye* detection. We present here an alternative solution using our film balance expansions induced by readily accessible simple calixarene building blocks, embedded in a monolayer over protein solutions in the lower nanomolar range ($10^{-8}-10^{-9}$ M).

Since each protein reacts differently with the receptor units **1**, **2**, **3**, or mixtures thereof embedded in the monolayer, the synopsis of all induced effects creates a recognition pattern, which is then specific for each individual protein (Figure 16). For example, histone H1 and cytochrome *c* are both very basic proteins with a similar expansive effect on the tetraphosphonate-doped monolayer (**1**). However, they react markedly different as soon as the anilinium halfsphere is added (**3** and **1**+**3**); now, histone H1 leads to much larger p/A shifts than does cytochrome *c*. Similarly, thrombin and BSA are both essentially neutral proteins, with quite comparable effects on monolayers containing only **1** or **3**. As soon as **1** and **3** are combined, BSA appears to be superior in its affinity toward the monolayer. Thus, each column in the graphical representation in Figure 16b constitutes

(43) This corresponds well with ESI-MS measurements carried out by Coleman et al. on the related complex between BSA and tetrasulfonatocalixarenes: Memmi, L.; Lazar, A.; Brioude, A.; Ball, V.; Coleman, A. W. *Chem. Commun.* **2001**, 2474−2475.
(44) Kodadek, T. *Chem. Biol.* **2001**, *8*, 105−115.
(45) Zhu, H.; Snyder, M. *Curr. Opin. Chem. Biol.* **2001**, *5*, 40−45.
(46) Boder, E. T.; Midelfort, K. S.; Wittrup, K. D. *Proc. Natl. Acad. Sci. U.S.A.* **2000**, *97*, 10701−10705.
(47) de Wildt, R. M. T.; Mundy, C. R.; Gorick, B. D.; Tomlinson, I. M. *Nat. Biotechnol.* **2000**, *18*, 989−994.
(48) Hesselberth, J.; Robertson, M. P.; Jhaveri, S.; Ellington, A. D. *Rev. Mol. Biotechnol.* **2000**, *74*, 15−25.

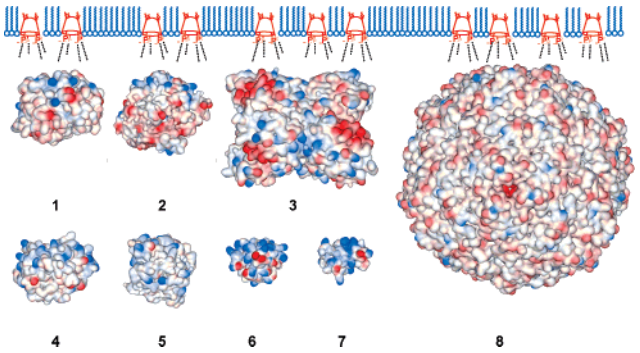

Figure 17. Proteins, which are bound by receptor **1** in the stearic acid monolayer, are depicted in their correct relative sizes. The Connolly surface is patterned with the electrostatic surface potential (ESP), showing basic and acidic domains on the protein surfaces. The basic proteins are shown in their proposed orientation relative to the monolayer, presenting their positive domains (blue) upward. **1** Proteinase K, **2** thrombin, **3** BSA, **4** chymotrypsin, **5** trypsin, **6** cytochrome *c*, **7** histone H1, and **8** ferritine.

a fingerprint of the respective protein, reflecting its different interactions with anionic (**1**), cationic (**2**), mixed polar (**3**), or zwitterionic (**1**+**3**) self-assembled monolayers. Very simple, in gram quantities readily accessible building blocks thus allow the specific and quantitative detection of proteins at nanomolar concentrations.

Outlook. A valuable tool for the identification of protein surface areas suitable for interaction with the tetraphosphonate receptor is the EPS (electrostatic potential surface). In Figure 17, the examined proteins are depicted in their correct relative sizes with a Connolly surface[49] and the typical EPS color code (blue = positive charge, red = negative charge). Apparently, those proteins with a large flat surface area covered with arginines and lysines are optimal binding partners for the lipid/tetraphosphonate monolayer. If only one such domain exists, the protein molecules must be oriented parallel to each other in order to dock onto the anionic binding sites on the monolayer "ceiling". The biological function of such a protein will be blocked if the active center is located just within this basic domain (e.g., α-chymotrypsin).[50] Thus, it should be possible to identify active centers and to interfere with the natural catalytic processes of basic proteins by docking them onto monolayers with immobilized arginine and lysine binders. The positively charged pendant to our new host system should be able to recognize acidic proteins and nucleic acids at very low concentrations. Since protein molecules with uniformly charged domains will be oriented along the surface, their crystallization might be facilitated.[51] We will carry out experiments along these lines soon. Similar to former experiments with self-assembled nucleotide receptors,[52] we will also try to combine, in a combinatorial manner, various amphiphilic calixarene receptors with recognition motifs for different classes of amino acids inside the monolayer to obtain a higher specificity for certain selected proteins (molecular patterning; hydrophobic residues might, e.g., be efficiently recognized by the starting material tetrakis[*tert*-butyl]calix[4]arene). These readily available receptor cocktails should greatly enhance the sensitivity and selectivity of the doped monolayers for specific proteins.

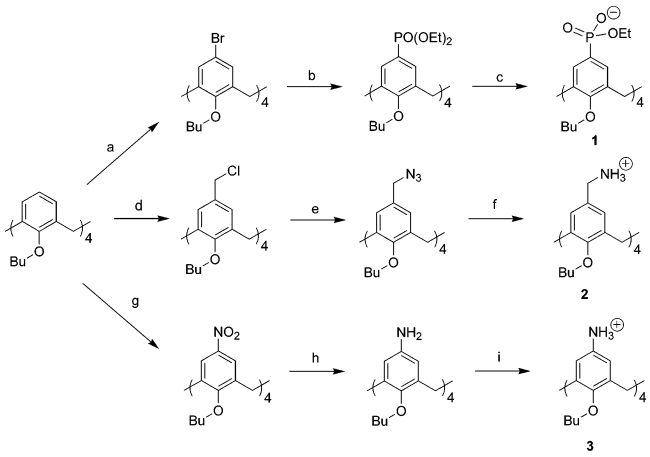

Figure 18. Synthetic route to the calix[4]arene halfspheres **1**, **2**, and **3**. (a) NBS, 75%. (b) $NiCl_2$, $P(OEt)_3$, 62%. (c) LiBr, 90%. (d) chloromethyloctyl ether, $SnCl_4$, 75%. (e) NaN_3, 86%. (f) HCl, 100%. (g) HNO_3, H_2SO_4, 65%. (h) H_2, Pd/C, 89%, (i) HCl, 100%.

Experimental Section

General Remarks. DMSO-d_6 (Aldrich), deuterium oxide (Merck), and methanol-d_4 (Merck) were each purchased in ≥99.8% purity. Thin-layer chromatography (TLC) analyses were performed on silica gel 60 F_{254} (Merck) with a 0.2 mm layer thickness. Preparative chromatography columns were packed with silica gel 60 from Aldrich. All solvents were dried and freshly distilled before use.

Synthesis of Calix[4]arene Receptors 1, 2, and 3. The synthesis of the anionic halfsphere starts with the 4-fold electrophilic bromination of the parent calixarene in its p-position, followed by halogen−metal exchange and subsequent reaction with electrophiles. With a Ni(II) catalyst and triethyl phosphite, the aromatic phosphonate was obtained; after that, a mild ester cleavage of the phosphonate ethyl ester was brought about by nucleophilic attack with LiBr in a dipolar aprotic solvent. The anilinium compound becomes accessible by nitration and subsequent catalytic hydrogenation (Figure 18).

Chloromethylation and subsequent S_N2 reaction led to a number of benzylic-substituted calixarenes. Depending on the choice of the nucleophile, this route offers access to amines (via azides), and protonation with dilute HCl completes the synthesis of the another cationic building blocks.

3,5-Bis(dimethoxyphosphorylmethyl)-1-hexadecanoic Acid Phenyl Amide. Quantities of 30 mg of 3,5-bis(dimethoxyphosphorylmethyl)-1-aminobenzene[53] (89 mmol, 1.0 equiv) and 26 mg of hexadecanoic acid (101 mmol, 1.1 equiv) were dissolved in 30 mL of dry dichloromethane. To this solution were added 77 μL of T3P (52% in ethyl acetate, 134 mmol, 1.5 equiv) and 20 μL of *N*-methylmorpholine (178 mmol, 2.0 equiv). The reaction was monitored by TLC. After 12 h, the solvent was evaporated, and the remaining yellow oil was separated by column chromatography on silica (10:1 dichloromethane/methanol). Yield: 47 mg (82 mmol, 92%). ^{1}H NMR (200 MHz, $CDCl_3$): δ 7.41 (s, 2H, CH-aromatic), 6.92 (s, 1H, CH-aromatic), 3.66 (d, $^3J_{P,H}$ = 10.8 Hz, 12H, P−O−CH_3), 3.10 (d, $^2J_{P,H}$ = 21.7 Hz, 4H, P−CH_2), 2.69 (t, $^3J_{H,H}$ = 6.9 Hz, 2H, NOC−CH_2−), 2.03 (m, 2H, OC−CH_2−CH_2−), 1.42 (s, 25H, alkyl chain), 1.12 (t, $^3J_{H,H}$ = 6.3 Hz, −CH_3). ^{31}P{^{1}H} NMR (81 MHz, $CDCl_3$): δ 29.1.

3,5-Bis(methoxyphosphorylmethyl)-1-hexadecanoic Acid Phenyl Amide Dilithium Salt, 1b. To a solution of 20 mg of 3,5-bis-(dimethoxyphosphorylmethyl)-1-hexadecanoic acid phenyl amide (35 mmol, 1.0 equiv) in 30 mL of dry acetonitrile was added 3.0 mg of

(49) (a) Connolly, M. L. *Science* **1983**, *221*, 709. (b) Connolly, M. L. *J. Appl. Crystallogr.* **1983**, *16*, 548.
(50) (a) Wei, Y.; McLendon, G. L.; Hamilton, A. D.; Case, M. A.; Purring, C. B.; Lin, Q.; Park, H. S.; Lee, C.-S.; Yu, T. *Chem. Commun.* **2001**, 1580−1581. (b) Park, H. S.; Lin, Q.; Hamilton, A. D. *J. Am. Chem. Soc.* **1999**, *121*, 8−13.
(51) Pechkova, E.; Nicolini, C. *J. Cell. Biochem.* **2002**, *85*, 243−251.
(52) For FMN recognition by a mixed monolayer, see: Ariga, K.; Kamino, A.; Koyano, H.; Kunitake, T. *J. Mater. Chem.* **1997**, *7*, 1155.
(53) Kim, Y.-C.; Jacobson, K. *J. Med. Chem.* **2000**, *43*, 746−755.

dry lithium bromide under argon. The solution was heated to reflux for 24 h. The white precipitate was filtered off and washed several times with acetonitrile. After drying under vacuum, 16 mg of the dilithium salt (29 mmol, 82%) remain. ^{1}H NMR (300 MHz, methanol-d_4): δ 7.24 (s, 2H, CH-aromatic), 6.92 (s, 1H, CH-aromatic), 3.40 (d, $^3J_{P,H}$ = 10.1 Hz, 6H, P−O−CH_3), 2.83 (d, $^2J_{P,H}$ = 20.8 Hz, 4H, P−CH_2), 2.23 (t, $^3J_{H,H}$ = 7.3 Hz, 2H, NOC−CH_2−), 1.58 (m, 2H, OC−CH_2−*CH_2*−), 1.18 (s, 25H, alkyl chain), 0.80 (t, $^3J_{H,H}$ = 6.6 Hz, −CH_3). ^{31}P{^{1}H} NMR (81 MHz, methanol-d_4): δ 26.2.

^{1}H NMR Titrations. Ten NMR tubes were filled each with 0.80 mL of a solution of the guest compound (c_{guest} = 0.5−4 mM) in a deuterated solvent (DMSO, CD_3OD, or D_2O). The host compound (1.525 equiv corresponding to the guest) was dissolved in 0.61 mL of the same solvent, and the resulting solution was added in amounts increasing from 0 to 5.0 equiv to the 10 guest solutions. Owing to their strong hygroscopicity, the phosphonate solutions contained approximately 0.3−0.6% water. Volume and concentration changes were taken into account during analysis. The association constants were calculated by nonlinear regression methods.

Job Plots. Equimolar solutions (10 mmol/10 mL, approximately 10 μM) of both the amino acids and the tetraphoshonate were prepared and mixed in various ratios. ^{1}H NMR spectra of the mixtures were recorded, and the chemical shifts were analyzed by Job's method modified for NMR results.

Molecular Modeling. Force-field calculations were initially carried out as molecular mechanics calculations in water. To establish the minimum energy conformation of the free host and guest molecule, as well as their 1:1 complex, Monte Carlo simulations were subsequently carried out in water (MacroModel 7.0, Schrödinger Inc., 2000. force field: Amber*). A 3000-step Monte Carlo simulation was performed. All low-energy structures were of very similar energy (ΔE ~5 kJ/mol) and conformation.

Film Balance Experiments. A NIMA 601BAM film balance (trough size 700 × 100 mm^2) equipped with a Wilhelmy plate was used for measuring the surface pressure as a function of molecular area at ambient temperature. Pure water (purified by ELGA Purelab UHQ, >18MΩ) and aqueous 100 μM amino acid solutions or 10 nM protein solutions were used as subphases, all of which did not give any appreciable values of surface pressure under compression in the examined area ranges. Lipid monolayers were obtained by spreading 50 μL of a 3.5 mM stearic acid solution in chloroform onto the subphases. The recorded π-A isotherm cycles (barrier speed = 50 cm^2/min) revealed no or only small isotherm changes of the stearic acid monolayer caused by dissolved guests (amino acids or proteins). Receptor **1** was incorporated into the lipid monolayer by dropping 5 μL of a 4.6 mM receptor solution in chloroform/methanol (1:1) onto the subphase at a surface pressure of 15 mN/m. Time-dependent π-A isotherm cycles were recorded until no further effects could be observed. The same procedure was followed in the presence of 50 mM NaCl or HEPES buffer (Figure 19).

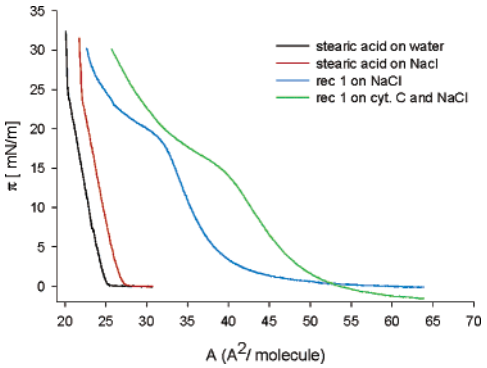

Figure 19. A p/A diagram detailing the individual interactions of NaCl (50 mM) with stearic acid, embedded calixarene **1**, and subinjected cyt *c* (10^{-8} M).

Langmuir−Blodgett Experiments. Monolayers at the air−water interface were prepared as described above with 0.1 or 0.4 equiv of receptor **1** and 0.2 equiv of receptor **2** embedded in the stearic acid phase. LB films were prepared on quartz plates (∅ = 1 cm, d = 1 mm) by the vertical dipping method at a controlled surface pressure of 20 mN/m with a dipping rate of 10 mm/min. Thus, 80 layers were deposited on each side of the plate. UV−vis spectra were recorded on a Hitachi U-3410 spectrometer at ambient temperature. The quartz plates were placed vertically in the optical path of the UV−vis spectrometer and measured directly in the range of 200−600 nm at ambient temperature. The free receptor molecules, **1** and **2** (150 μM), and free proteins, cytochrome *c* and BSA (25 μM), were prepared as aqueous solutions. Samples were measured in quartz cuvettes (d = 1 cm) as solution in pure water (purified by ELGA Purelab UHQ, >18MΩ).

For further experimental details, see the Supporting Information of the following Communication: Zadmard, R.; Arendt, M.; Schrader, T. *J. Am. Chem. Soc.* **2004**, *126*, 7752−7753.

Acknowledgment. This work was supported by the Deutsche Forschungsgemeinschaft. Protein samples were generously provided by the groups of M. Marahiel, L.-O. Essen, and G. Klebe (Marburg, Germany). Free samples of T3P were generously donated by Clariant GmbH (Frankfurt, Germany).

JA045785D